Carbon-based nanodots as effective electrochemical sensing tools towards the simultaneous detection of bioactive compounds in complex matrices

Cristina Montes[a,b], M. Laura Soriano[a,b], M. Jesús Villaseñor[a,c], Ángel Ríos[a,b]*

[a]Department of Analytical Chemistry and Food Technology, Faculty of Chemical Science and Technology, University of Castilla-La Mancha, 13071, Ciudad Real, Spain

[b]Regional Institute for Applied Chemistry Research (IRICA), 13071, Ciudad Real, Spain.

[c]Department of Analytical Chemistry, Industrial Engineering School, University of Castilla-La Mancha, 13071, Ciudad Real, Spain

* Corresponding Author. E-mail address: Angel.Rios@uclm.es

Abbreviations

CNDs: Carbon nanodots

CQDs: Carbon quantum dots

GQDs: Graphene quantum dots

TEM: Transmission electron microscopy

FTIR: Fourier transform infrared spectroscopy

Vit: Vitamin

SPCEs: Screen printed carbon electrodes

DPV: Differential pulse voltammetry

Nf: Nafion

k^0: Electron transfer rate constant

A: electroactive area

Cdl: double-layer capacitance

GO: Graphene oxide

BPPGE: Basal-plane pyrolytic graphite electrode

GCE: Glassy carbon electrode

AA: Ascorbic acid

UA: Uric acid

DA: Dopamine

L-tyr: L-tyrosine

Abstract

A comparative study about the electroanalytical performance of three types of carbon-based nanodots has been accomplished. They exhibit similar functionalities (oxygenated groups) but diverse size and core structure (morphology, crystallinity and quantum confinement): carbon nanodots (CNDs), carbon quantum dots (CQDs) and graphene quantum dots (GQDs), herein employed as potential sensing modifiers on screen printed electrode surface. All of them were top-down synthetized, as well as characterized by TEM, FTIR, Raman and fluorescence techniques. Their electrochemical properties were assessed by cyclic voltammetry using specific redox probes (outer and inner sphere systems), such as potassium hexacyanoferrate(III), hexaammine-ruthenium(III) chloride and dopamine, which display different electron transfer rate as a function of their electronic core structure and specific active sites. The electroanalytical capabilities of these carbogenic nanodots as suitable sensing tools towards the simultaneous detection of several bioactives like vitamins (ascorbic acid or Vit C, pyridoxine or Vit B2, riboflavin or Vit B6) and amino acids (cysteine and tyrosine), were also evaluated and discussed attending to the main interactions responsible for improvement in peak currents and potentials. Finally, GQD-based electrodes, selected as the best choice, were submitted to an exhaustive electroanalytical performance characteristics evaluation. The success of this simple drop-casting procedure was also proved by affording the simultaneous detection of three diverse bioanalytes in complex commercial matrices and with lower detection limits in comparison to other reported proposals from similar nature.

Keywords: carbon nanodots; carbon quantum dots; graphene quantum dots; electrochemical sensing; bioactive analytes.

1. Introduction

Screen-printed electrodes are still unceasingly garnering considerable attention as a transducer for electroanalysis in comparison to conventional electrode materials, as far as being low-cost, disposable, portable, reproducible and reliable sensors [1] as well as enabling analysis of very small sample volume as miniaturized devices. Their potential in (bio)analytical applications to selectively preconcentrate target analytes on electrode surface and to improve sensitivity is maximized upon their versatility to be modified by a variety of nanomaterials [2, 3]. It is noteworthy that surface modification with carbonaceous inks painted onto the conductive tracks has gained much attention. In fact, recent works focused on the fabrication and functionalization of carbon conductive inks from chemically inert carbon materials (high mechanical resistance, electrical and thermal conductivity) with binding components and/or additives for a further use as screen-printed electrodes' modifiers to detect a variety of target (bio)analytes [4 - 6], although the inclusion of them usually slows down the electron rate. Graphene and carbon nanotubes had been also incorporated directly into the manufacturing inks [7, 8], however, they suffered from heterogeneity and low reproducibility due to aggregation and stacking effects.

Amongst carbon allotropes, carbon-based nanodots are considered as a green alternative by virtue of their non-toxicity, biocompatibility, high water solubility and their ability to exchange electrons [9]. Our aim lies to understand the electrochemical activity of these carbon-based nanodots, which remains controversial, since until now most studies have been mainly focused on their optical properties [10, 11]. The present research is specifically focused on SPCEs (screen printed carbon electrodes) modification with different types of carbon-based nanodots [12 - 16] displaying tunable properties with

regard electron transfer, quantum confinement, electrical conductivity, and surface area for improving the transduction of electrochemical signals of (bio)sensing devices. Although the combination of carbon-based nanodots and SPCEs have been previously reported, limitations in terms of sensitivity and reproducibility were found [15, 17].

Carbon-based nanodots are a new family of spherical dots (size below 30 nm) [9] which are overall categorized into graphene quantum dots (GQDs), carbon quantum dots (CQDs) and carbon nanodots (CNDs). On one side, they possess unique physicochemical properties such as stable fluorescence, large specific surface area and surface grafting, but on the other hand, they can differ by their crystallinity, graphitized-core degree (sp^2/sp^3 hybridization), morphology and quantum confinement. Thus, these differences in their cores entail diverse electrochemical activities and photoluminescence behaviors. Crystalline laminar GQDs display quantum confinement effects and a crystalline structure unlike spherical CNDs. Spherical CQDs exhibit some structural heterogeneity (sp^2 and sp^3 hybridization) and, consequently, an intermediate degree of crystallinity [9]. Such nanodots have been revealed as powerful tools in the fabrication of sensors, energy generation and storage devices [18, 19].

Because of their certain similarity degree about some features (e.g. diameter range, solubility, oxygen containing groups, photoluminescence properties), the mechanisms involving both their photoluminescence and electrochemical activity are still in debate. Whereas many efforts were focused over their photoluminescence mechanisms enabling us to distinguish amongst the nanodot types and surface passivation [10, 11, 20], there is a lack of comparative electrochemical studies which makes difficult to understand the corresponding involved electrochemical mechanisms [21, 22]. From the above, there is a need about these systematic and comparative works addressing the electrochemical

properties exhibited by these different carbon-based nanodots obtained by a variety of synthetic routes, with diverse core, etc. and the subsequent role they play in electron transfer kinetics too [23]. So far, just few specific reviews devoted to electrochemical applications of carbon nanostructures have been found in literature [24 - 27].

This work pretends to give readers a deep comparative insight about the electrochemical behavior of GQDs, CQDs and CNDs containing similar functionalized surface (oxygenated groups), but different crystallinity, core hybridization, morphology, and quantum confinement. With this aim the three families were firstly synthesized following the top-down methodology and later thoroughly characterized both structural and electrochemically by means of well-known redox probes, surface sensitive in different degree to its chemistry and microstructure [28]. Thus, this study has been directed toward the understanding of those factors controlling carbon dots electrochemistry overall and their heterogeneous transfer rate specifically, in an attempt to gain perspective for a rational design of different carbon-based electrodes with implemented analytical performance as a function of specific analytes.

The electroanalytical capabilities of these carbon nanodots-electrodes as sensing electrochemical modifiers are also evaluated versus a set of significant bioactive target analytes, namely vitamins (Vit B2, Vit B6 and Vit C) and amino acids (*L*-tyrosine). Primary interactions responsible for their shifts in peak potentials and their increase in peak currents were also elucidated. Finally, attending to its valuable electrochemical features, modified GQD-SPCEs were selected to carry out the simultaneous detection of these bioactives in commercial nutritional supplements by differential pulse voltammetry (DPV). The present research tries to open new possibilities for the design and tailoring of sensing systems attending the specific chemistry of the sought analyte.

2. Experimental

2.1. Reagents and solutions

All aqueous solutions were prepared with analytical grade reagents and deionized water purified with a Milli-Q system (Millipore, Bedford, MA, USA) that reaches a resistivity of 18.2 MΩ·cm at 25°C. Pyridoxine (≥ 98%), riboflavin (≥ 98%), *L*-tyrosine (≥ 98%), *L*-cysteine (≥ 97%), potassium ferricyanide (≥ 99%), potassium chloride (≥ 99%), hexaammineruthenium(II) chloride (≥ 99%), dopamine hydrochloride (≥ 98%), sodium hydroxide (≥ 98%), methanol (≥ 99%), sodium phosphate dibasic (≥ 99%), sodium phosphate monobasic (≥ 99%), sodium carbonate (≥ 99.5%), potassium chloride (≥ 99%), sulfuric acid (95 - 97%) and cellulose microcrystalline (50-mm particles) and dialysis tubing-bags (3500 kDA cut off) were purchased from Sigma-Aldrich. were acquired from Sigma-Aldrich (St. Louis, MO, USA). Acetone (0.01% water content), ascorbic acid (≥ 99%) and fuming hydrochloric acid (37%) were purchased from Panreac (Badalona, Spain). Nitric acid (≥ 69%) was supplied by Labkem (Mataró, Barcelona, Spain). Nafion 117 (Nf, 5% mixture of aliphatic alcohols and water) was supplied by Fluka (Steinheim, Germany). Multiwalled carbon nanotubes and graphene were purchased from Bayer and Nanomaterials Avanzare Innovation technology S.L., respectively.

Stock standard solutions of potassium ferricyanide, dopamine hydrochloride and hexaammineruthenium(II) chloride (0.005 M) were prepared in KCl (0.1 M). Pyridoxine, ascorbic acid, and *L*-cysteine were prepared in deionized water, *L*-tyrosine in HCl (1M) and riboflavin in a mixture of water/methanol (20%). All solutions were stored in darkness at low temperature until use.

Different electrolyte solutions were prepared by dissolving/diluting appropriate amounts of reagents and adjusting to suitable pH values with HCl (0.1M) and NaOH (0.1M). Working solutions were daily prepared by diluting stock solutions in the corresponding electrolyte buffer solutions.

Commercial samples of Mincartil, Vitax and *L*-Tyrosine BioTech were acquired in local supermarkets from well-known brands. Recommended daily amounts of each nutritional supplement: Mincartil (3 capsules, 3.0367 g) and Vitax (1 capsule, 1.5 g) were crushed and dissolved in deionised water (50 mL for Mincartil and 10 mL for Vitax). Daily amounts of *L*-Tyrosine BioTech (2 capsules, 1.154 g) were dissolved in 25 mL of 1M HCl. Next, the samples were shaken by vortex, sonicated for one hour and filtered. Finally, solutions were prepared as follows using the corresponding electrolyte until 2 mL of final volume: 40% KCl (0.1 M) for Mincartil sample, 40% HNO_3 (0.05 M) for Vitax and 80% KCl (0.1 M) *L*-Tyrosine BioTech, all of them v/v and 50 µL of each one were submitted to the voltammetric procedure.

2.2. Instrumentation

Electrochemical experiments were performed with a CHI842D electrochemical analyzer controlled by Chi842d software from CH Instruments (Austin, Texas USA). Measurements were carried out with a three-electrode cell configuration, using screen printed (modified) carbon electrodes (SPCEs, DRP-110) from Dropsens (Oviedo, Spain) consisting of a carbon counter electrode, a silver pseudo reference electrode and a carbon working electrode (4 mm diameter). A DRP-BICAC70311 connector was used as interface between the potentiostat unit and the screen-printed electrode.

The morphology of the carbonaceous nanodots were examined by transmission electron microscopes (TEM) using a JEOL JEM 1400 and JEOL 2100 (high resolution) models. For sample preparation, aliquots of the diluted sample were placed in a TEM grid and air dried before the analysis.

Raman scattering behaviours of samples were evaluated with an InVia Renishaw microspectrometer selecting a laser of 532 nm. Data was collected in triplicate and treated with origin software. The Raman samples were prepared from stable dispersions of the nanodots. Diluted solutions of them were deposited dropwise over a silica oxide plate and air dried at 40ºC before the analysis.

Photoluminescence of CNDs, CQDs, GQDs solutions were characterized measuring the emission at the maximum excitation wavelengths for each carbon-based nanodots in aqueous media. A PTI QuantaMasterTM spectrofluorometer was used with a 2 nm-set up of excitation and emission slit widths and 10 mm quartz cuvettes. All measurements were performed in triplicate.

Infrared spectra of the solid samples were conducted in a crystal Attenuated Total Reflectance (ATR) for Shimadzu Infrared (IR) instrument (ATR crystal puck was of ZnSe, IR-Affinity-1S model and DTGS Standard detector).

An ultrasound bath (Selecta, Barcelona, Spain) and a Basic 20 pH-meter with a combined glass electrode (Crison Instruments S.A., Barcelona, Spain) were also used.

2.3. Synthesis of CNDs, CQDs and GQDs

CNDs, CQDs and GQDs were synthesized according to previously reported methods [29, 30]. Briefly, CNDs were prepared from cellulose microcrystalline (1 g) in an acidic

solution (H_2SO_4, 12.2 N) under reflux conditions for 7 h. CQDs and GQDs were synthesized from multiwalled carbon nanotubes (0.2 g) and graphene (20 mg) as carbon precursors at 140 ºC in presence of an acidic mixture (H_2SO_4/HNO_3, 3:1 ratio) for 7.5 and 5 h, respectively. Passivation of their surfaces was carried out with acetone (5 mL) overnight. All the residues were treated with sodium carbonate and the resulted suspensions were subjected to centrifugation (13000 r.p.m.) to isolate the respective nanodots from the supernatant. Once all bigger particles and aggregates were removed, the carbon-based nanodots were subsequently purified with ethanol at low temperatures to remove excess of salts by crystallization. Finally, these latest ethanolic solutions containing the respective nanomaterials were dried, reconstituted in deionized water and subjected to dialysis for 4 h.

2.4. Carbon-based nanodots surface modification procedure on carbon SPCEs

Solutions containing 2 $g \cdot L^{-1}$ of each carbon-based nanodots in 5% v/v Nafion (CND/Nf, CQD/Nf and GQD/Nf) were prepared by sonication (15 min). Then, three aliquots (5 µL each one) of the previous solutions were subsequently drop-casted onto the working electrode letting to dry between depositions under IR lamp. After that, the modified electrode surface was rinsed with deionized water before use. From now on, these electrodes modified with CND/Nf, CQD/Nf, and GQD/Nf solutions will be referred to as CND-SPCEs, CQD-SPCEs and GQD-SPCEs, respectively.

2.5. Electrochemical procedure

Electrochemical characterization of the bare and modified SPCEs as sensing devices was performed through cyclic voltammetry (CV) at different scan rates using three redox probes, namely $[Ru(NH_3)_6]Cl_3$, $K_3Fe(CN)_6$ and dopamine (5 mM in 0.1 M KCl).

Electroanalytical studies of vitamins and amino acids were carried out by DPV using the modified SPCEs by dilution of appropriate amounts of analyte stock solutions in different electrolytes; 0.1 M KCl for dopamine, ascorbic acid, cysteine and tyrosine and 0.05 M HNO_3 for riboflavin and pyridoxine. To check target compounds, 50 µL of the sample were deposited onto the electrode surface; then CV and DPV voltammograms were recorded under potential ranges from -0.7 to 0.9 V and from –1.0 to 1.4 V, respectively. DPV instrumental conditions were as follows: increment potential 4 mV, amplitude 250 mV, pulse width 0.05 s, sampling width 0.02 s, pulse period 0.6 s and quiet time 2 s. All electrochemical experiments were performed at room temperature.

2.6. Theoretical calculations for electrochemical parameters

The potential difference (ΔE_p) for each electrode surface is obtained from the following equation:

$$\Delta E_p = E_{p,a} - E_{p,c} \qquad (1)$$

where Ep_a and Ep_c are the anodic and cathodic peak potentials, respectively. This parameter provides information about the electrochemical reversibility of a redox couple.

The electron transfer rate constant ($k^{0'}$) lets to know the rate at which redox exchange occurs. The electron transfer rate constant of each electrode is achieved following the Nicholson method [31]:

$$\Psi = k^{0\prime} \cdot (D_O/D_R)^{\alpha/2} \cdot (RT)^{1/2} \cdot (\pi nFDv)^{-1/2} \qquad (2)$$

where D_O and D_R are diffusion coefficients for oxidized and reduced species ($cm^2 \cdot s^{-1}$), respectively, α is the transfer coefficient, R and F are the universal constant of gasses ($J \cdot mol^{-1} \cdot K^{-1}$) and Faraday constant ($C \cdot mol^{-1}$), respectively, T is absolute temperature (K),

n is number of exchanged electrons, and *v* is the scan rate ($V \cdot s^{-1}$). Upon the approximation $D_O/D_R = 1$, the equation (2) resulted to be as follows:

$$\Psi = k^{0\prime} \cdot (RT)^{1/2} \cdot (\pi n F D v)^{-1/2} \quad (3)$$

The dimensionless function (Ψ) was calculated for each scan rate according equation (4) previously described by Swaddle [32], using as ΔE_p its respective value for a specific scan rate:

$$Ln\,\Psi = 3{,}69 - 1{,}16 \cdot Ln(\Delta E_p - 59) \quad (4)$$

Afterwards, $k^{0'}$ is calculated from the slope of expression (3) by plotting the previous obtained Ψ values versus the square root of *v*.

The electroactive area (*A*) of each electrode is estimated from Randles-Sevcik equation [33]:

$$i_p = 2{,}69 \cdot 10^5 \cdot n^{3/2} \cdot A \cdot C \cdot D^{1/2} \cdot v^{1/2} \quad (5)$$

where i_p is the peak current, *n* is the number of exchanged electrons, *A* the electroactive area of electrode (cm^2), *C* is analyte concentration ($mol \cdot cm^{-3}$), *D* are the diffusion coefficients of ruthenium, ferricyanide and dopamine: $9.1 \cdot 10^{-6}$, $7.6 \cdot 10^{-6}$ and $1.4 \cdot 10^{-5}$ $cm^2 \cdot s^{-1}$, respectively, and *v* is the scan rate ($V \cdot s^{-1}$). All *A* values, depicted in **Table 1**, are calculated from the slope resulted by plotting cathodic peak current versus square root of *v*.

The double capacitance layer *(Cdl)* is calculated using the following equation:

$$i_c = A \cdot Cdl \cdot v \quad (6)$$

where i_c is the capacitive current (μA), *A* is area of electrode, *v is* the scan rate ($V \cdot s^{-1}$) being *Cdl* units of $\mu F \cdot cm^{-2}$. Once known the calculated electrode area, the capacitance value for each electrode is obtained from the slope by plotting i_c versus *v*.

3. Results and discussion

3.1. Nanostructural characterization of CNDs, CQDs and GQDs

Obtained sizes by TEM were quite similar for the three nanostructures, with the smallest diameter for CQDs (3 nm ± 0.32), followed by CNDs (7 nm ± 0.18) and the largest one for GQD (9 nm± 0.27) (**Fig. 1.A, 1.B and 1.C**). By FTIR, the three carbon-based nanodots display similar functional groups on the surface (oxygenated groups). In particular, bands found at ca. 3500 and 1700 cm^{-1} are typically ascribed to the stretching vibrational modes of the hydroxyl (O-H) and carbonyl (C=O) bonds, which likely involve the presence of carboxyl groups. These oxygenated groups are responsible of their high solubility in water (**Fig. 1.D, 1.E and 1.F**). Anyway, from the intensity associated to these bands it can be supposed a more successful passivation for CNDs and GQDs than for CQDs. On the other hand **Fig. 1.G** and **1.H** showed the Raman profiles of the graphitic/graphenic nanodots (CQDs and GQDs), which are alike in appearance and characteristic of graphenic structures with their typical features including both G (≈1585 cm^{-1}, crystalline) and D (≈1380 cm^{-1}, disorder) modes, which confirmed the sp^2 hybrids carbons at basal planes and the symmetry breaking at edges and defects with existence of sp^3 carbons. No clear bands at the 2D region (≈2800 cm^{-1}) were detected, as occurred for this type of nanodots since their defective nature provokes deactivation of the 2D effect with the thickness variation [34]. Regarding the CNDs, lack of any representative Raman profile was obtained as result of their amorphous structure.

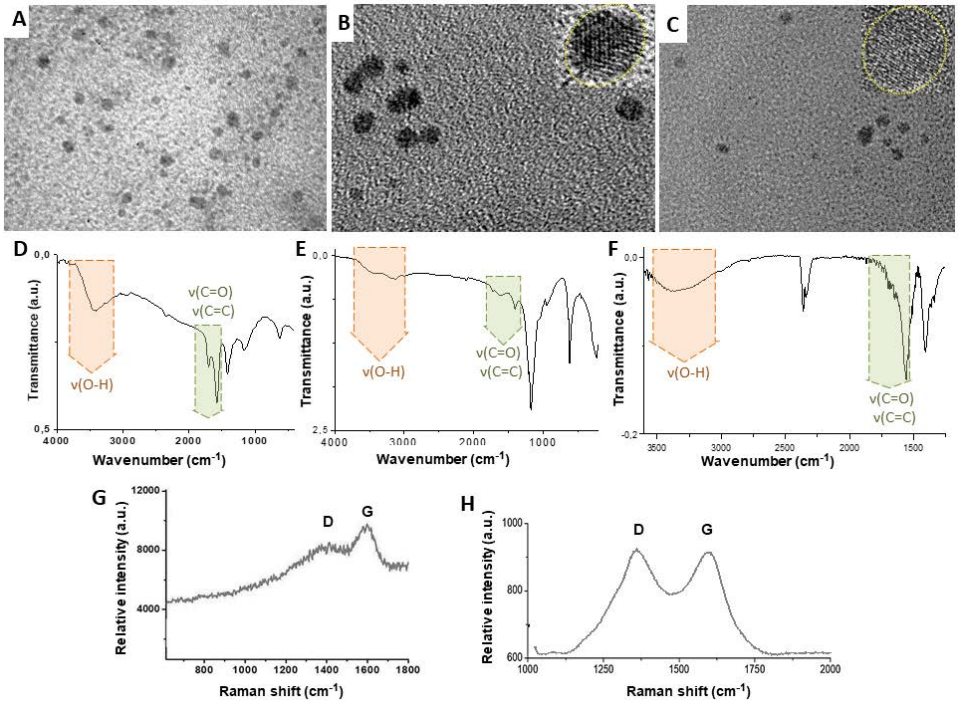

Fig. 1. Micrograph images of CNDs (**A**), CQDs (**B**) and GQDs (**C**) with the inter lattice spacing of 0.269 nm (illustrative insets); IR spectra of CNDs (**D**), CQDs (**E**) and GQDs (**F**); Raman shifts of CQDs (**G**) and GQDs (**H**).

All three nanodots showed excellence fluorescence properties with excitation (370 nm, 350 nm and 350 nm) and emission (450 nm, 455 nm and 470 nm) for CQDs, CNDs and GQDs respectively (**Fig. 2**), wavelengths suggesting the lowest quantum confinement effects for GQDs which involved better electronic conductivity properties, in disagreement with consulted literature [23], but in accordance with the sp^2-carbon hybridization assigned to graphenic layers. In addition, the emission wavelength resulted to be pH dependent for CQDs and GQDs aqueous solutions (more pronounced for the former ones) (**Fig. 2.A, 2.B and 2.C**), likely due to the band gap structure of their aromatic domains, responsible of the quantum confinement.

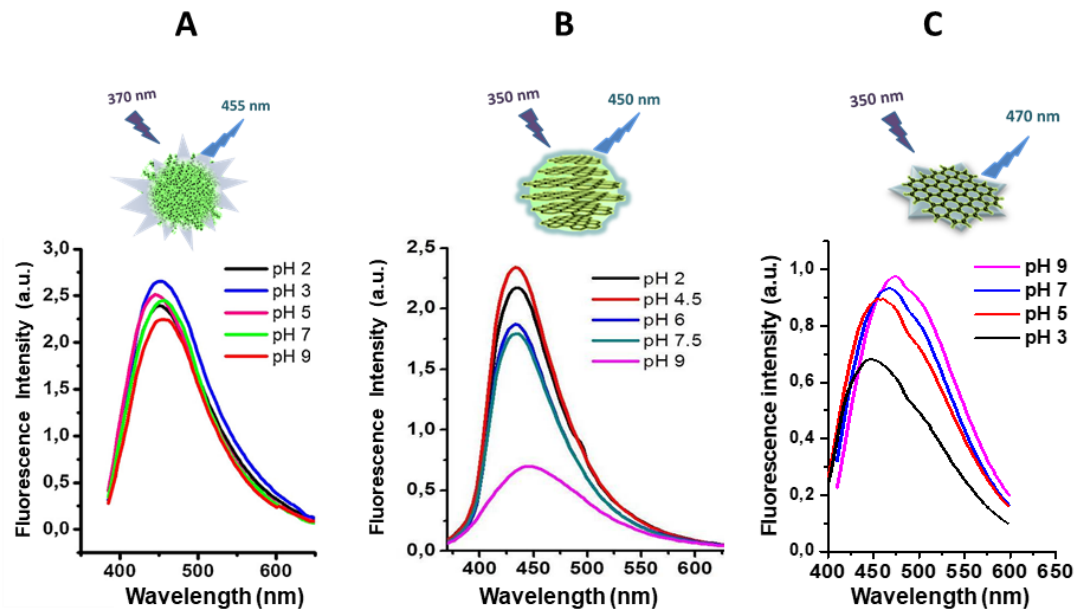

Fig. 2. Illustration of the emission and excitation features of CNDs (**A**), CQDs (**B**) and GQDs (**C**) and their emission behaviour versus the pH of the medium.

3.2. Selection of conditions for electrode surface modification

To select the best conditions for carbon-based nanodots modification on electrode surface, different experiments were carried out addressing the concentration of the modifiers (carbon-based nanodot), the Nafion percentage as well as the number and volume of depositions. All these experiments were performed by CV (scan rate: 100 $mV \cdot s^{-1}$) for a 5 mM dopamine in 0.1 M KCl solution. Firstly, the influence of CNDs, CQDs and GQDs concentration (2, 10 and 20 $g \cdot L^{-1}$) to modify the electrode was evaluated. As shown in **Fig. 3A**, the concentration range studied did not produce any significant change in the observed current for any of carbon nanodots; therefore, 2 $g \cdot L^{-1}$ was chosen as a suitable concentration for the electrode modification.

Secondly, different methodologies were tried to select the suitable volume and number of depositions for electrode modification: in one of them, a single aliquot was drop-casted

but testing two different volumes (30 and 15 µL) and allowing to dry this surface under an IR lamp. It was observed that the increase of drop volume did not provide any gain in terms of current results. Attending to the obtained current and handling aspects, 15 µL were selected as suitable volume. In a second methodology, the selected volume (15 µL) was added by three depositions (5 µL each one) with the same drying process. The latter deposition method provided the best results for the carbon modifiers handling, being selected for the electrode modification. This was due to the high water-solubility of nanodots, which promoted a very rapid expansion of each released drop along and beyond the working electrode surface, covering even the two remaining electrodes and hindering their use so.

To avoid this drawback, the polymeric membrane Nafion was used as a binder between these carbon-based nanodots and the working electrode. **Fig. 3B** displays the obtained current values for the bare electrode and for the modified ones in the absence and presence of Nafion (5% v/v). It was found that modified electrodes without Nafion already had greater sensitivity than the bare one. Interestingly, when adding Nafion these electrochemical responses significantly improved for the 3 modified surfaces being the CND/Nf electrode that displayed the best results. In short, Nafion led to better current results and solved the drop expansion problem already mentioned.

Then, the Nafion influence on electron transfer kinetic and reversibility behavior was also evaluated by means of ΔEp (**Fig. 3C**). This study showed that CND/Nf and GQD/Nf surfaces provided very remarkable smaller values than the other modified ones and then, exhibited greater reversibility. Lastly, the Nafion percentage in modifiers mixtures was checked (0.5%, 2.0% and 5.0% v/v). From these experiments, 5% was selected as the ideal percentage for the three nanodot species attending to the obtained current as well as

the greater drop density thus facilitating any supposed electrode manufacturing process (**Fig. 3D**). All cyclovoltamograms obtained during the optimization process are shown in **Fig. S1**.

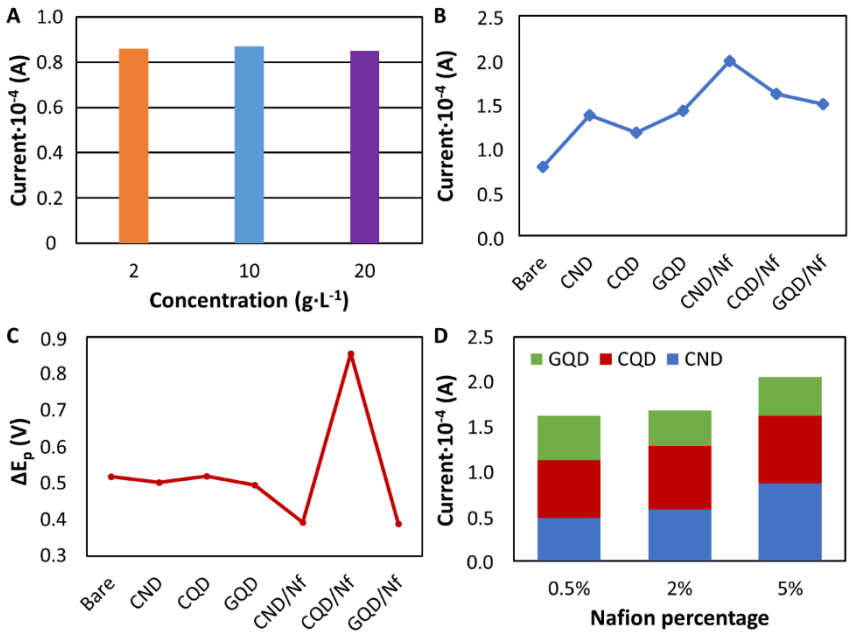

Fig. 3. Selection of conditions for modifying electrode surface (5 mM dopamine in 0.1 M KCl): Oxidation peak current versus different CNDs nanodot concentrations (**A**); Oxidation peak current (**B**) and ΔEp (**C**) for the bare SPCEs and for the modified ones with and without Nafion; Nafion percentage study for the modified carbonaceous nanodot SPCEs (**D**).

It is noteworthy by means of the performed experiments to optimize surface modification process and unlike other previously reported works [8], it was checked the absence of stacking or agglomeration effects for any nanodot dispersions into the electrode surface thanks to their high water solubility from the layer edges (passivation), even for CQD and GQDs and despite their sp^2-framework.

3.3. Electrochemical characterization of CNDs, CQDs and GQDs

With the aim to perform the electrochemical characterization of the three nanodots, three representatives redox probes, well known as outer and inner sphere in different degree [28], namely hexaammineruthenium(III) chloride, ferricyanide and dopamine, were

checked in an attempt to get insights about both their electrochemistry and nanostructure. As relevant parameters of this electrochemical study at electrode surface their reversibility, heterogeneous kinetic rate constant, electroactive area (*A*) and capacitance were evaluated at scan rates from 10 to 500 $mV \cdot s^{-1}$ by CV with the bare and modified CND/Nf, CQD/Nf and GQD/Nf electrodes.

Before starting this elucidating study, the working potential windows for these modified electrodes were checked by performing background "blank" CV scans. **Fig. S2** displays the resultant profile for a KCl 0.1 M solution (pH 7) in the three electrodes, exhibiting comparable featureless voltammograms in a wide range, from – 0.6 to 1.0 V, that means their electrochemical suitability as sensing modifiers and especially for anodic processes.

Since hexaammineruthenium(III) chloride complex is well-documented as an outer-sphere redox probe sensitive to electron state density [28] but not to surface chemistry of the electrode surface, it was used to evaluate the relationship between edges and basal planes for spherical random carbon core (CND), stacked graphitic sheets forming a sphere (CQD) and individual single sheet (GQD) electrode. According to diverse authors [8, 28], the *A* and electron transfer rates for Ru complex do not change from the surface chemistry but upon the electrode´s electronic structure (Fermi levels and density of states), here mainly depending of ratio edge plane sites and defects. The analysis of voltammetric profiles assessed upon this redox probe was mainly based on the heterogeneous electron transfer rate constant ($k^{0'}$) and electroactive area (*A*) values, since the results in terms of potential difference (ΔE_p) have not provided relevant information; in fact similar values were achieved, namely 179, 173 y 172 mV for CND/Nf, CQD/Nf and GQD/Nf electrodes respectively. In terms of rate-limiting step (diffusion and/or adsorption), both processes were evaluated by representing the peak currents against the scan rate and the square root

of scan rate. Results suggested that the kinetic of the electrochemical process at the CND/Nf, CQD/Nf and GQD/Nf electrodes are mainly controlled by the diffusion of electroactive species through the electrode surface owing to a linearly peak current dependency with the square root of scan rate. Considering $k^{0'}$, calculated by Nicholson method [31], CND/Nf electrode displays the better rate-limiting step with a value $7.5 \cdot 10^{-4}$ cm·s^{-1} followed by the GQD/Nf electrode with $5.3 \cdot 10^{-4}$ cm·s^{-1}. Since these voltammetric responses correlates with the proportion of edge and basal planes, it can be deduced that content of edges plane and defects plane is higher for the CND/Nf electrode whilst CQD/Nf and GQD/Nf electrodes have higher contents of basal plane which is consistent with their graphitized nanosheet-containing cores. Regarding the electroactive area (*A*), calculated with such near-ideal outer-sphere probe by the Randles-Sevcik equation [33], the CND/Nf modified electrode gave the best results too, followed by the GQD/Nf one (**Table 1**).

Persisting in the characterization of these three electrodes, an inner-sphere redox probe, ferricyanide complex, surface-sensitive but no oxygenated groups-sensitive, was used to evaluate the effect from the different surface morphologies (spherical, stacked sheets and isolated sheets) since this probe requires a steric interaction with the adsorbed nanodots layers for electron transfer [28]. As the previous redox probe, ferricyanide also exhibits a reversible behavior and the electronic transfer control takes place by diffusion, therefore, this is the limiting step. CND/Nf electrode is the one that shows a smaller potential difference (69 mV) and a higher kinetic constant ($4.18 \cdot 10^{-3}$ cm·s^{-1}), meaning that kinetic transfer is more favored for the amorphous core nanostructure with spherical shape, (refereed as to CNDs) than for the other two sp^2-composed crystalline frameworks. These results suggest a higher content/accessibility of defectives sites in the CND surface (i.e.

carbonyl groups) [28, 35], thus evidencing the improved electrocatalytic activity for a non-graphitic electrode morphology in nature.

Finally, it was used a second inner-sphere probe, dopamine, both surface and oxygen sensitive, whose electrochemical response can reveal the variety of attached functional groups to the nanodot surfaces owing to a set of non-covalent interactions: the electrostatic interaction of the positively-charged amine of the redox probe toward the negatively-charged carboxyl groups of the nanodots reinforced by hydrogen bonding and the π-π interactions towards graphitic/graphenic nanodots. Taking into account that, upon the previous FTIR characterization of three nanodot types similar surface moieties (namely, carboxyl and hydroxyl groups) are attached to diverse carbon cores (amorphous and sp^2 carbon frameworks or sheet), the achieved electrochemical results are in agreement with this since the peak potentials obtained for the three surfaces are very similar; in short, this peak potential appears at 0.65 V for both GQD/Nf and CQD/Nf electrodes whilst it moves slightly forward (ca. 20 mV) for CND/Nf electrode. About the kinetic constant, both CND and CQD possess a similar transfer rate ($5.3 \cdot 10^{-4}$ cm·s^{-1} and $5.6 \cdot 10^{-4}$ cm·s^{-1}, respectively), while a slightly higher value ($6.9 \cdot 10^{-4}$ cm·s^{-1}) was observed for GQDs. It is noteworthy to highlight that, in terms of rate electron transfer constant and *A*, the three carbonaceous structures exhibited better results compared to the bare electrode, noting that the GQD/Nf electrode displayed the best electrocatalytic effect toward dopamine attending to the $k^{0'}$ and ΔEp values. This is possibly due to π-π stacking interactions which are mainly responsible of this behavior, besides the high content of oxygen superficial groups enhancing electrostatic interactions with it (nanostructural characterization section).

All commented electrochemical parameters for the three modified electrodes and the bare one with the three redox probes are summarized in **Table 1.**

CVs related to the evaluation of $k^{0'}$ and A for the three tested redox probes are given as **Figs. S3**, **S4** and **S5** for $[Ru(NH_3)_6]Cl_3$, $K_3[Fe(CN)_6]$ and dopamine, respectively. Each figure also contains the corresponding graphical fits used for calculating $k^{0'}$ (Ψ versus $v^{-1/2}$) and *A* (Ip_c versus $v^{1/2}$) from their slopes for each one of the carbonaceous nanodot electrode.

Besides, the corresponding CVs and graphical fits relative to Cdl calculations for the tested redox probes on each carbonaceous modified electrode are included by means of **Fig. S**6.

Table 1. Electrochemical characterization related to the three carbon-based nanodots.

Probe	Electrode	$k^{0'}$ ($cm \cdot s^{-1}$)	A (cm^2)	Cdl ($\mu F \cdot cm^{-2}$)
$[Ru(NH_3)_6]^{3+}$	**Bare**	$1.68 \cdot 10^{-3}$	0.110	53
	CNDs/Nf	$7.48 \cdot 10^{-4}$	0.171	688
	CQDs/Nf	$3.29 \cdot 10^{-4}$	0.067	6517
	GQDs/ Nf	$5.33 \cdot 10^{-4}$	0.089	2291
$[Fe(CN)_6]^{3-}$	**Bare**	$1.11 \cdot 10^{-3}$	0.135	49
	CNDs/ Nf	$4.18 \cdot 10^{-3}$	0.021	5000
	CQDs/ Nf	$3.74 \cdot 10^{-3}$	0.013	33846
	GQDs/ Nf	$3.80 \cdot 10^{-3}$	0.021	10000
Dopamine	**Bare**	$1.60 \cdot 10^{-4}$	0.010	47230
	CNDs/ Nf	$5.27 \cdot 10^{-4}$	0.030	1743
	CQDs/ Nf	$5.63 \cdot 10^{-4}$	0.025	6452
	GQDs/ Nf	$6.85 \cdot 10^{-4}$	0.019	9231

$k^{0'}$ (electron transfer rate constant); A (electroactive area); Cdl (double-layer capacitance).

To elucidate which electrochemical mechanisms are undertaken for each of the three redox probes used in these nanodot-modified SPCEs, the following observations can be considered:

According to the influence from: *i)* the nanodot surface (several oxygenated functional groups), in which the ferricyanide probe displays for CNDs a higher electron transfer rate in comparison to those graphitized nanodots likely due to the high accessibility of defective sites (superficial oxygenated moieties) on its spherical surface, thus also enhancing electrostatic interactions with dopamine (high *A*); *ii)* the nanodot core (different nanostructures and carbon hybridization degrees), where both *A* and electron transfer rate were higher for the amorphous CNDs when the outer-sphere redox probe ruthenium complex was checked, suggesting so a higher density of electronic states, here related with ratio edge plane sites and defects (possibly from carbonyl bonds) at this electrode surface; *iii)* specific interactions with dopamine, where GQD/Nf electrode displays the higher electron transfer rate as a result of the electrostatic interactions between the carboxyl nanosheets and the cationic dopamine reinforced by π-π interactions which contributed more extensively than the other non-covalent forces previously mentioned.

As concluding remarks of these experience, the modification of SPCE with such nanodots clearly introduces carbon-oxygen functionalities, which has been proved by better electrochemical dopamine responses, besides an increase of reactive edge plane sites and defects, with a great influence on electron transfer kinetic and *A*, especially for CND/Nf and GQD/Nf (attending to electrostatic and π-π interactions).

3.4. Electrochemical study of relevant biological molecules on CND-SPCEs, CQD-SPCEs and GQD-SPCEs

DPV was the chosen technique to investigate the electrochemical response of such nanodots as sensing modifiers versus relevant biological molecules like vitamins (namely, ascorbic acid, riboflavin and pyridoxine) and amino acids (e.g. tyrosine and cysteine) usually very common in a wide variety of nutritional commercial supplements.

The sensing of these essential dietary components is of great importance to define and check the limits of dosages for consumer safety in nutritional supplements, since over their legal limits these components may provoke potential negative side effects. Thus quick, economic, and sensitive methods for vitamins and amino acids detection are required to assure product quality with an efficient legal and regulatory compliance. Currently, liquid chromatography is the most extended technique for simultaneous determination of vitamins in a variety of matrices. Herein, we open a cheap and accurate possibility for their simultaneous determination in dietary supplements after the valuable electrochemical characterization and application of the three studied carbon-nanodots.

DPV profiles of target compounds are depicted in **Fig. 4** using KCl (0.1 M) as electrolyte for ascorbic acid, tyrosine, and cysteine, and HNO_3 (0.05 M) for riboflavin and pyridoxine.

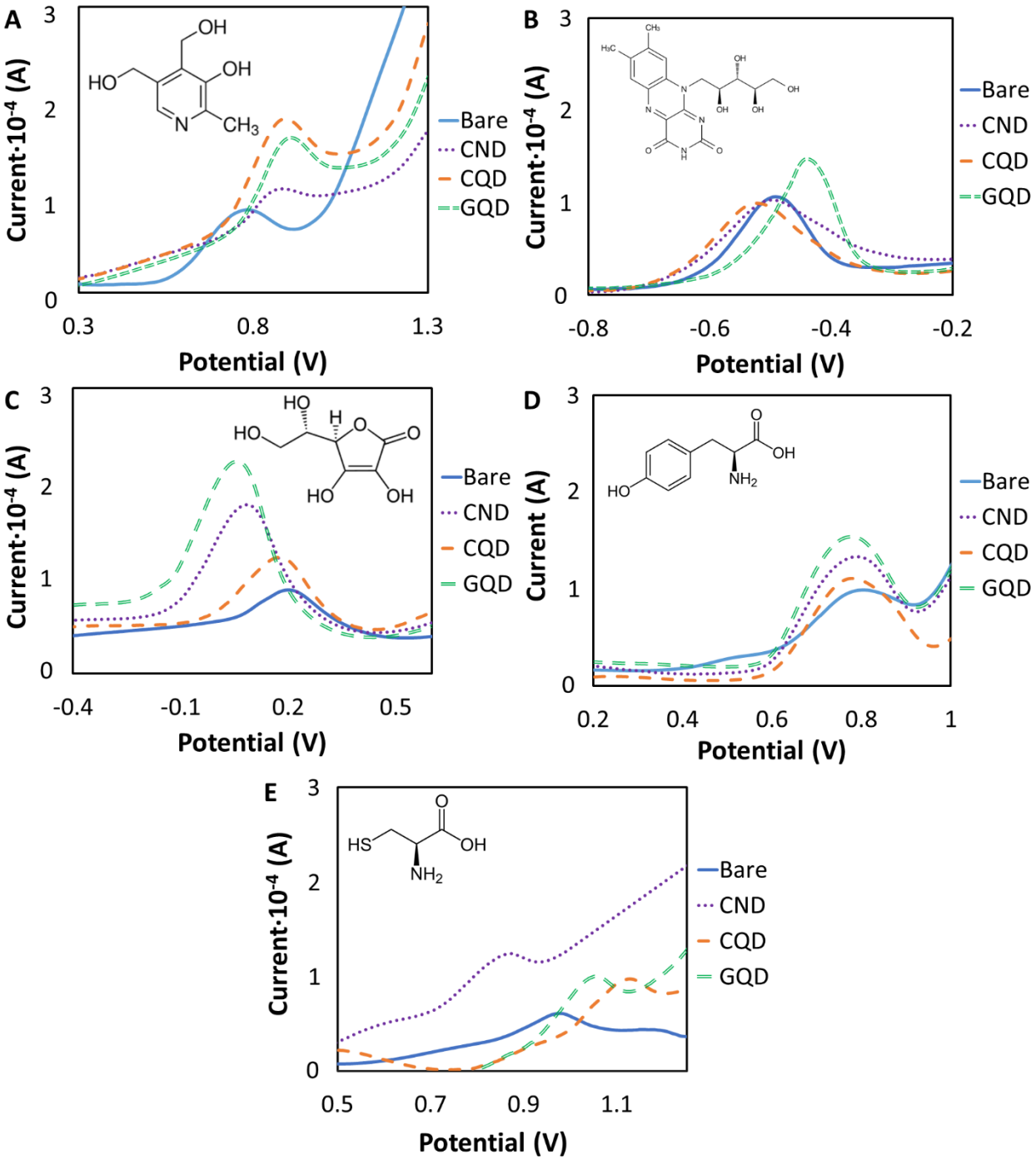

Fig. 4. DPV profiles of CND/Nf, CQD/Nf and GQD/Nf electrodes for 1 mM pyridoxine (**A**), 0.3 mM riboflavin (**B**), 5 mM ascorbic acid (**C**), 1 mM tyrosine (**D**) and 5 mM cysteine (**E**). Electrolyte for **A** and **B** was 0.05 M HNO_3 and 0.1 M KCl for **C**, **D** and **E**.

As it can be seen, all CQD/Nf, CND/Nf and GQD/Nf electrodes showed higher oxidation peak currents than the bare electrode for all molecules; of special interest is the detection of riboflavin, in which a markedly high peak current was found for GQD/Nf in

comparison to CQD/Nf and CND/Nf electrodes which displayed oxidation peak currents similar to the bare one. These results agree with the higher conductivity of the single graphenic layer in GQD owing to the sp^2-carbon hybridization. It should be highlighted that GQD/Nf electrode is the one presenting a better electrochemical behavior in terms of better sensitivity and/or shifting potentials of the target analytes for their detection, especially for riboflavin and ascorbic acid. In relation to vitamin C detection, two important aspects came out: *i)* it was possible to increase the sensitivity, and *ii)* the oxidation of the analyte moved to a lower potential value. Overall, the relevant degree of oxidation of the modified surface is a key factor for promoting the hydrogen bonding with the target analytes. In addition, the sp^2 framework seems to play an important role for enhancing the π-π interactions with the aromatic rings of such organic molecules resulting in higher intensity signals. Interestingly, vitamins B2 and B6 containing electron-deficient heterocycles interacted strongly to those electrode surfaces based on graphitized nanodots (e.g. pyridoxine peak is more intense for CQD and GQDs whilst riboflavin peak is more intense for GQDs). Regarding ascorbate, the voltammetric response was strongly dependent on the electrode modification, finding that the anodic peak potential appeared at higher intensity for GQD as well as exceptionally shifted its potential to forward values (very close 0 V). Attending to checked literature [36], it is due to the charge transfer from the 2-furanone derivative to the graphenic nanolayers which acted as a better electron acceptor. In the detection of cysteine, the peak intensity was still low although it was improved compared to the bare one; besides, it is better defined and forwarded in the CNDs electrode. Overall, these results indicate the importance of hydrogens bonding (caused by surfaced oxygenated functionalities) and the π-π interactions (from graphenic nanosheets) as main contributions to enhance the detection of various targeted molecules.

This behavior is shown in **Fig. 5** that illustrates the interactions of GQD on the electrode surface and riboflavin and ascorbic acid as representative analytes.

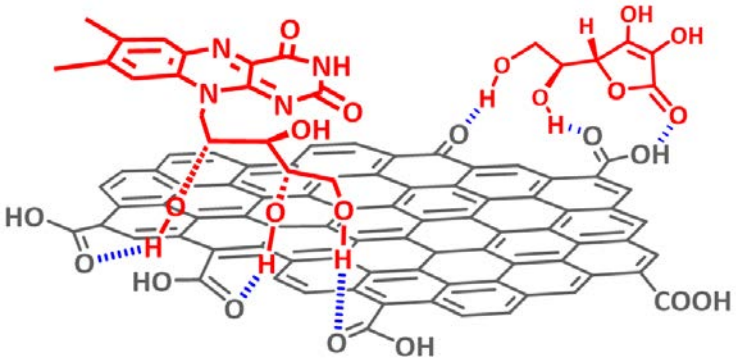

Fig. 5. Schematic illustration of the possible interactions between riboflavin and ascorbic acid (red) and GQDs electrode surface (grey). Hydrogen bonds and π-π interactions are depicted in blue and green, respectively.

3.5. Electroanalytical performance characteristics

Concerning some of these relevant biological analytes, figures of merits were evaluated to check the electroanalytical capabilities of these carbon nanodots-electrodes as sensing electrochemical modifiers by their application in real samples.

Firstly, precision of the three modified electrodes was evaluated by means of repeatability and reproducibility studies of both current and potential peak values for the electrochemical sensing of riboflavin and tyrosine as target analytes. The obtained results are displayed in **Table 2**.

Table 2. Repeatability and reproducibility results for the electrochemical sensing of riboflavin and tyrosine.

Repeatability		n	GQD	CQD	CND
Riboflavin	Current	9	2.8	3.2	3.4
	Potential	9	1.3	1.1	1.4
Tyrosine	Current	9	8.8	7.0	9.1
	Potential	9	0.4	0.8	0.7
Reproducibility		**n**	**GQD**	**CQD**	**CND**
Riboflavin	Current	4	0.9	3.1	1.4
	Potential	4	0.7	1.9	1.9
Tyrosine	Current	4	3.3	4.6	6.5
	Potential	4	1.0	0.8	1.2

Concerning repeatability (same electrode, n=9), the relative standard deviation (RSD) values about potential peak for riboflavin were excellent, between 1.1 and 1.4%, while for tyrosine were in the range of 0.4 - 0.8%, which was especially meaningful with the perspective of simultaneous targets sensing. Reproducibility studies (four electrodes, n=4) provided RSD values in the ranges of 0.7% - 1.9% and 0.8% - 1.2% for riboflavin and tyrosine, respectively. These results evidenced the good precision of the electrodes considering a potential manufacturing process (batch-to-batch evaluation).

The linear behavior was checked for the electrochemical sensing of riboflavin, ascorbic acid, and tyrosine in KCl 0.1 M using the GQD/Nf screen printed electrode (**Fig. 6**), achieving the following linear fits:

Riboflavin $I_p = [1.94 \cdot 10^{-5} \pm 4.47 \cdot 10^{-6}] + [3.96 \cdot 10^{-3} \pm 8.93 \cdot 10^{-5}] \cdot C(mM)$ $r^2 = 0.997$

Ascorbic acid $I_p = [1.39 \cdot 10^{-5} \pm 1.78 \cdot 10^{-7}] + [9.90 \cdot 10^{-6} \pm 2.31 \cdot 10^{-7}] \cdot C\ (mM)$ $r^2 = 0.997$

Tyrosine $I_p = [-1.23 \cdot 10^{-5} \pm 8.44 \cdot 10^{-7}] + [6.30 \cdot 10^{-5} \pm 1.04 \cdot 10^{-6}] \cdot C\ (mM)$ $r^2 = 0.999$

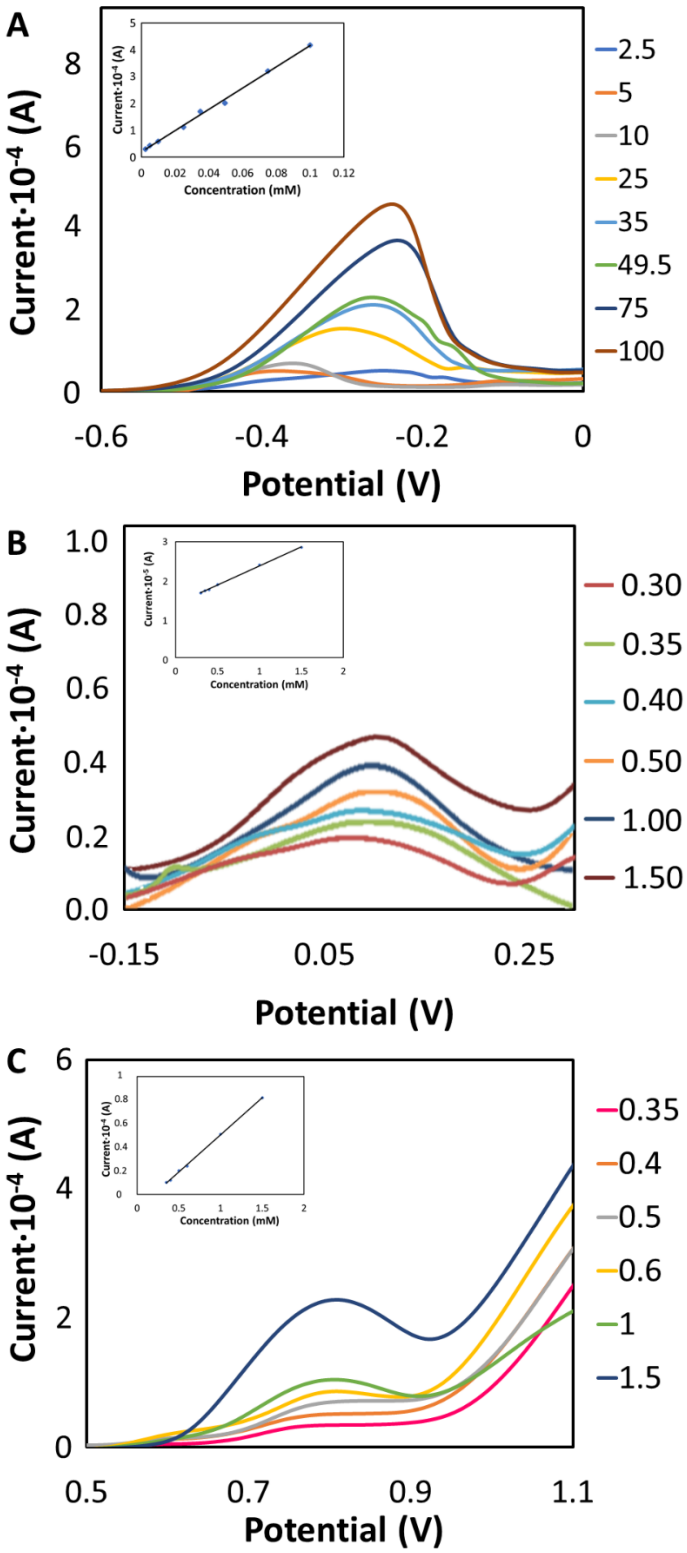

Fig. 6. DPV responses and calibration plots (insets) of riboflavin (**A**), ascorbic acid (**B**) and tyrosine (**C**).

Detection limits (LOD) for riboflavin, ascorbic acid and tyrosine were found to be of 0.83 µM, 0.1 mM and 0.12 mM respectively, whereas their corresponding quantification limits

(LOQ) were 2.50 μM, 0.30 mM and 0.35 mM, respectively. Initially, these parameters were calculated according to IUPAC criterion, being LOD the blank signal plus three times its standard deviation and LOQ the blank signal plus ten times its standard deviation. Then, both limits were adjusted experimentally getting lower LOD and LOQ values. Reached LOD values were significantly lower than other previously reported using similar carbon nano-based sensing materials (**Table 3**).

Table 3. Comparative evaluation of the proposed method amongst other carbon-based electrochemical sensing approaches.

Type of electrode	Electrode modification	Analytes	Electroanalytical performance	Simultaneous detection	LOD (mM)	Samples	Ref.
SPCE	-Graphene	Ascorbic acid (AA) Uric acid (UA) Dopamine (DA)	LOD Linearity	No	0.35 (AA) No reported	No	[8]
BPPGE[a]	-CQDs -GQDs	Ascorbic acid (AA) Uric acid (UA)	Qualitative	No	No reported No reported	No	[23]
GCE[b]	-Graphene oxide (GO) nanoribbons -Reduced GO nanoribbons	Ascorbic acid (AA) Uric acid (UA) Dopamine (DA)	Qualitative Precision	Yes	0.50 (AA) 0.05 (UA) 0.05 (DA)	Yes	[34]
		L-tyrosine (L-tyr) Uric acid (UA)			1.0 (UA) 1.0 (L-Tyr)		
SPCE	-GQDs	Riboflavine (Rib) Ascorbic acid (AA) *L*-tyrosine (L-Tyr) Pyridoxine	Linearity Lower LOD, LOQ Precision	Yes	$8.3 \cdot 10^{-4}$ (Rib) 0.10 (AA) 0.12 (L-Tyr)	Yes	This work
	-CQDs -CNDs			No			

[a] BPPGE: Basal-plane pyrolytic graphite electrode; [b] GCE: Glassy carbon electrode

3.6 Application to commercial nutritional supplements

Attending to the electrocatalytic behavior displayed by the three modified nanodots electrodes, the GQD/Nf one was selected to attain the simultaneous detection of three vitamins (C, B2 and B6) in the commercial nutritional supplement Vitax, of two vitamins (C, B2) and tyrosine in the supplement Mincartil and of tyrosine in the commercial sports supplement L-Tyrosine BioTech. In all cases, the working samples were prepared upon advices of their recommended daily amounts (section “Reagents and solutions”).

The DPV profiles of Mincartil, Vitax and L-Tyrosine BioTech samples are depicted in **Fig. 7**, finding RSD values (n=5) for riboflavin (Mincartil) of 4.2 (I_p) and 3.1% (E_p), for ascorbic acid (Vitax) of 1.6 (I_p) and 1.1% (E_p),and for tyrosine (L-Tyrosine Biotech) of 4.6 (I_p) and 0.7 % (E_p), respectively.

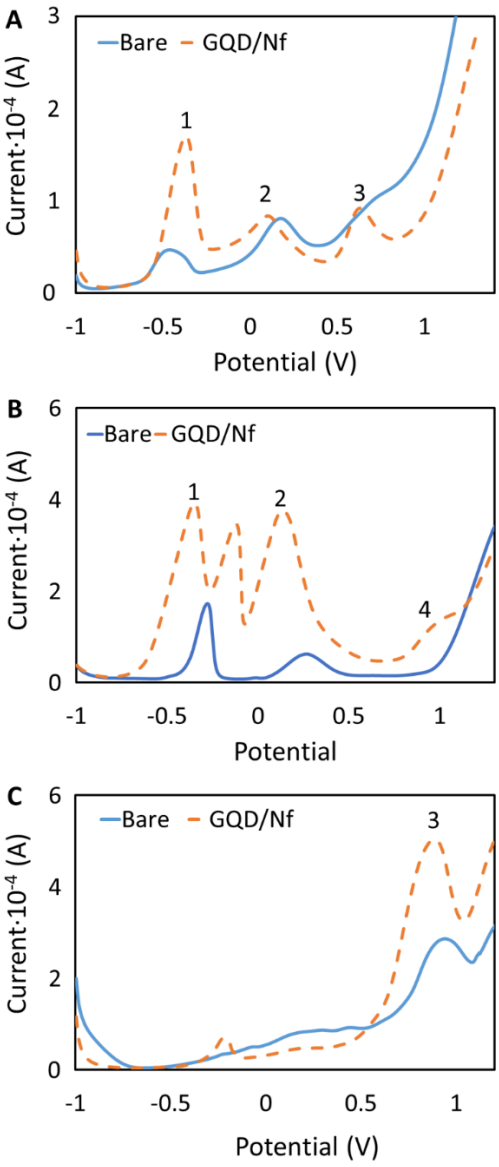

Fig. 7. Voltammograms for Mincartil in 0.1 M KCl (**A**), Vitax in 0.05 M HNO_3 (**B**) and L-tyrosine BioTech (**C**) in 0.1 M KCl using the GQD/Nf electrodes. Peaks marked as 1, 2, 3 and 4 refer to the analytical signal of riboflavin, ascorbic acid, tyrosine, and pyridoxine, respectively.

Many of these molecules are usually oxidized at very close potentials; then, discrimination between these species in a mixture can be extremely difficult. Herein, this point has been successfully afforded since riboflavin, ascorbic acid and tyrosine peaks were especially well-resolved by this simple approach.

Thus, GQDs have proved to be an excellent modifier of SPCEs for the simultaneous electrochemical sensing of complex mixtures of target analytes from diverse nature in

commercial nutritional supplements. Thus, from the comparative evaluation displayed in **Fig. 5** for Mincartil and /or Vitax, it is observed that an increase in sensitivity and forwarded peaks are always achieved with the GQD electrode enabling even the electrochemical sensing of tyrosine and pyridoxine, very disabled in the bare one.

Furthermore, **Table 3** shows a comparison of the proposed GQDs sensing approach with other already existing carbon nano-based electrochemical ones, in which its advantages are evidenced in terms of simultaneous detection for diverse bioanalytes and lower LOD, among others.

4. Conclusions

This work has revealed the usefulness of modifying SPCE with the emerged carbon-based nanodots as potential analytical tools. Results showed diverse electrocatalytic activity for electrodes containing GQDs, CQDs or CNDs with same oxygenated superficial groups based on their ratio reactive edge-plane sites and defects in their respective cores. Differences were also found regarding the chemicophysical interactions responsible of the electrochemical sensing toward a variety of amino acids and vitamins as target molecules.

Remarkably, GQD-SPCE displayed an impressive electroanalytical performance attending to hydrogen bonding (oxidation degree) and π-π interactions, which was satisfactory applied for the simultaneous determination of several bioactives (vitamins B2, B6 and C and tyrosine) in nutritional supplements, discrimination that is usually difficult for their closer oxidation potentials. This point would enable even their simultaneous quantification, giving so an additional value to the proposal. Moreover,

LOD values obtained were significantly lower than other previously reported using similar carbon-based nanosensors.

This work offers then a rational survey about the electrocatalytic activity of diverse carbon-based nanodots from different nature affording advantages in the electrode preparation (by simple drop-casting modification of the SPCEs) with a good batch-to-batch reproducibility, which are of great consideration for their further potential manufacturing. With that research, we try to search new possibilities for the design of electrochemical sensors based on functionalized GQDs depending on the specific chemistry of various target analytes to find also an effective resolution of the mixtures in complex samples with an improved sensitivity.

Acknowledgements

This work was supported by the Spanish Ministry of Economy and Competitiveness (MINECO) [grant number PID2019-104381GB-I00] and JJCC Castilla-La Mancha [grant number JCCM SBPLY/17/180501/000262]. M. L. Soriano expresses her gratitude to both the European Commission and the JJCC Castilla-La Mancha for the funding project SBPLY/17/180501/000333.

References

[1] J. P. Metters, R. O. Kadara, C. E. Banks, New directions in screen printed electroanalytical sensors: an overview of recent developments, Analyst 136 (6) (2011) 1067-1076. https://doi.org/10.1039/C0AN00894J

[2] C. Pérez-Ràfols, N. Serrano, J. M. Díaz-Cruz, C. Ariño, M. Esteban, New approaches to antimony film screen-printed electrodes using carbon-based nanomaterials substrate, Analytica Chimica Acta 916 (2016) 17–23. https://doi.org/10.1016/j.aca.2016.03.003

[3] Y.-H. Wang, L.-L. He, K.-J. Huang, Y.-X. Chen, S.-Y. Wang, Z.-H. Liu, D. Li, Recent advances in nanomaterial-based electrochemical and optical sensing platforms for microRNA assays, Analyst 144 (2019) 2849-2866. https://doi.org/10.1039/C9AN00081J

[4] R. A. Dorledo de Faria, Y. Messaddeq, L. G. Dias Heneine, T. Matencio, Application of screen-printed carbon electrode as an electrochemical transducer in biosensors, Int. J. Biosen. Bioelectron. 5(1) (2019) 1–2. DOI: 10.15406/ijbsbe.2019.05.00143

[5] P. Nicholas, R. Pittson, J. P. Hart, Development of a simple, low cost chronoamperometric assay for fructose based on a commercial graphite-nanoparticle modified screen-printed carbon electrode, Food Chemistry, 241(2018) 122-126. https://doi.org/10.1016/j.foodchem.2017.08.077

[6] S. F. Chin, L. S. Lim, S. C. Pang, M. S.H. Sum, D. Perera, Carbon nanoparticle modified screen printed carbon electrode as a disposable electrochemical immunosensor strip for the detection of Japanese encephalitis virus, Microchimica Acta, 184 (2) (2017) 491–497. https://doi.org/10.1007/s00604-016-2029-7

[7] J. Ping, J. Wu, Y. Wang, Y. Ying, Simultaneous determination of ascorbic acid, dopamine and uric acid using high-performance screen-printed graphene electrode. Biosens. Bioelectron., 34 (2012) 70–76. https://doi.org/10.1016/j.bios.2012.01.016

[8] E. P. Randviir, D. A. C. Brownson, J. P. Metters, R. O. Kadara, C. E. Banks, The fabrication, characterization and electrochemical investigation of screen-printed graphene electrodes, Phys. Chem. Chem. Phys., 16 (2014) 4598-4611. https://doi.org/10.1039/C3CP55435J

[9] A. Cayuela, M. L.Soriano, C. Carrillo-Carrión, M. Valcárcel, Semiconductor and carbon-based fluorescent nanodots: The need for consistency, Chemical Communication, 52 (2016) 1311-1326. https://doi.org/10.1039/C5CC07754K

[10] A. Sciortino, A. Cannizzo, F. Messina, Carbon Nanodots: A Review—From the Current Understanding of the Fundamental Photophysics to the Full Control of the Optical Response. Journal of Carbon Research, 4 (2018) 67. DOI:10.3390/c4040067

[11] A. Sciortino, M. Gazzetto, M. L. Soriano, M. Cannas, S. Cárdenas, A. Cannizzo, F. Messina, Ultrafast spectroscopic investigation on fluorescent carbon nanodots: the role of passivation, Physical Chemistry Chemical Physics, 21 (2019) 16459-16467. https://doi.org/10.1039/C9CP03063H

[12] S. Zheng, R. Huang, X. Ma, J. Tang, Z. Li, X. Wang, J. Wei, J. Wang, A highly sensitive dopamine sensor based on graphene quantum dots modified glassy carbon electrode, Int. J. Electrochem. Sci., 13 (2018) 5723 – 5735. DOI: 10.20964/2018.06.19

[13] M. Algarra, A. González-Calabuig, K. Radotić, D. Mutavdzic, C.O. Ania, J.M. Lázaro-Martínez, J. Jiménez-Jiménez, E. Rodríguez-Castellón, M. del Valle, Enhanced

electrochemical response of carbon quantum dot modified electrodes, Talanta 178 (2018) 679–685. DOI: 10.1016/j.talanta.2017.09.082

[14] S. Gupta, T. Tyler Smith, A. Banaszak, Graphene quantum dots electrochemistry and development of ultrasensitive enzymatic glucose sensor, MRS advances, 3 (2018)15-16, 831-847. https://doi.org/10.1557/adv.2018.324

[15] J. Mehta, N. Bhardwaj, S. K. Bhardwaj, S. K. Tuteja, P. Vinayak, A. K. Paul, K.-H. Kim, A. Deep, Graphene quantum dot modified screen printed immunosensor for the determination of parathion, Analytical Biochemistry, 523 (2017) 1-9. https://doi.org/10.1016/j.ab.2017.01.026

[16] S. C. Tan, S. F. Chin, S. C. Pang, Disposable Carbon Dots Modified Screen Printed Carbon Electrode Electrochemical Sensor Strip for Selective Detection of Ferric Ions, Journal of Sensors, 1 (2017) 1-7. DOI: 10.1155/2017/7576345

[17] F. Valentini, D. Romanazzo, M. Carbone, G. Palleschi, Modified screen-printed electrodes based on oxidized graphene nanoribbons for the selective electrochemical detection of several molecules, Electroanalysis, 24 (4) (2012) 872 – 881. https://doi.org/10.1002/elan.201100415

[18] S. Benítez-Martínez, A. I. López-Lorente, M. Valcárcel, Determination of TiO_2 nanoparticles in sunscreen using N-doped graphene quantum dots as a fluorescent probe, Microchim. Acta, 183 (2016) 781–789. DOI:10.1007/s00604-015-1696-0

[19] A. Ambrosi, C. K. Chua, N. M. Latiff, A. H. Loo, C. H. A. Wong, A. Yong Sheng Eng, A. Bonanni, M. Pumera, Graphene and its electrochemistry – an update, Chem. Soc. Rev., 45 (2016) 2458. https://doi.org/10.1039/C6CS00136J

[20] A. Sciortino, A. Cayuela, M. L. Soriano, F. M. Gelardi, M. Cannas, M. Valcárcel, F. Messina, Different Natures of Surface Electronic Transitions of Carbon Nanoparticles, Physical Chemistry Chemical Physics, 19 (2017) 22670 - 22677. https://doi.org/10.1039/C7CP04548D

[21] K. Li, J. Xu, M. Arsalan, N. Cheng, Q. Sheng, J. Zheng, T. Yue, Nitrogen doped carbon dots derived from natural seeds and their application for electrochemical sensing, Journal of The Electrochemical Society, 166(2) (2019) B56–B62. DOI: 10.1149/2.0501902jes

[22] B. A. Sami, Nanostructured carbon electrode modified with N-doped graphene quantum dots–chitosan nanocomposite: a sensitive electrochemical dopamine sensor, R. Soc. open sci., 4 (2017) 171199. DOI: 10.1098/rsos.171199

[23] C. S. Lim, K. Hola, A. Ambrosi, R. Zboril, M. Pumera, Graphene and carbon quantum dots electrochemistry, Electrochemistry Communications, 52 (2015) 75-79. DOI: 10.1016/j.elecom.2015.01.023

[24] L.-M. Shen, J. Liu, New development in carbon quantum dots technical applications, Talanta, 156-157 (2016) 245–256. https://doi.org/10.1016/j.talanta.2016.05.028

[25] P. S. Sharma, F. D'Souza, W. Kutner, Graphene and graphene oxide materials for chemo- and biosensing of chemical and biochemical hazards, Top. Curr. Chem., 348 (2014) 237–265. DOI: 10.1007/128_2013_448

[26] P. Tian, L. Tang, K. S. Teng, S. P. Lau, Graphene quantum dots from chemistry to applications, Materials Today Chemistry, 10 (2018) 221-258. https://doi.org/10.1016/j.mtchem.2018.09.007

[27] F. Faridbod, A. L. Sanati, Graphene quantum dots in electrochemical Sensors/Biosensors, Current Analytical Chemistry, 15(2) (2019) 103-123. DOI:10.2174/1573411014666180319145506.

[28] P. Chen, R. L. McCreery, Control of electron transfer kinetics at glassy carbon electrodes by specific surface modification, Analytical Chemistry, 68(22) (1996) 3958-3965. https://doi.org/10.1021/ac960492r

[29] A. Cayuela, M. L. Soriano, M. Valcárcel, Photoluminescent carbon dots as sensors for carboxylated multiwalled carbon nanotube detection in river water, Sensors & Actuators B-chemical, 207 (2015) 596-601. https://doi.org/10.1016/j.snb.2014.10.102

[30] A. Cayuela, M. L. Soriano, M. Valcárcel, Strong luminescence of CDs induced by acetone passivation: Efficient sensor for a rapid analysis of two different pollutants, Analytica Chimica Acta, 804 (2013) 246-251. DOI: 10.1016/j.aca.2013.10.031

[31] R. Nicholson, Theory and application of cyclic voltammetry for measurements of electrode reaction kinetics, Anal. Chem., 37(1965) 1351-1355. https://doi.org/10.1021/ac60230a016

[32] T. W. Swaddle, Homogeneous versus heterogeneous self-exchange electron transfer reaction of metal complexes: insights from pressure effects, Chemical Reviews, 105 (6) (2005) 2573-608. https://doi.org/10.1021/cr030727g

[33] D. Martín-Yerga, E. Costa Rama, A. Costa García, Electrochemical study and determination of electroactive species with screen-printed electrodes, J. Chem. Educ., 93(7) (2016) 1270–1276. https://doi.org/10.1021/acs.jchemed.5b00755

[34] K. Sung, S. Dong Hee, K. Chang, K. Soo Seok, J. Soong, Ch. Suk-Ho, H. Sung Won and S. Cheolsoo, Size-dependence of Raman scattering from graphene quantum dots: Interplay between shape and thickness, Applied Physical Letters, 102, (2013) 53108 -53113. http://dx.doi.org/10.1063/1.4790641.

[35] M. R. Kagan, R. L. McCreery, Quantitative Surface Raman Spectroscopy of Physisorbed Monolayers on Glassy Carbon, Langmuir, 11 (1995) 4041-4047. https://doi.org/10.1021/la00010a068

[36] A. Martin, J. Hernández-Ferrer, L. Vazquez, M. Martínez, A. Escarpa, Controlled chemistry of tailored graphene nanoribbons for electrochemistry: a rational approach to optimize molecule detection, RSC Adv., 4 (2014) 132-239.
https://doi.org/10.1039/C3RA44235G